

## CFD Prediction of Solid Particle Distribution in Baffled Stirred Vessels under Partial to Complete Suspension Conditions

Alessandro Tamburini<sup>a,\*</sup>, Andrea Cipollina<sup>a</sup>, Giorgio Micale<sup>a</sup>, Alberto Brucato<sup>a</sup>,  
Michele Ciofalo<sup>b</sup>

<sup>a</sup>Dipartimento di Ingegneria Chimica, Gestionale, Informatica, Meccanica - Università degli Studi di Palermo, Viale delle Scienze Edificio 6 - 90128 Palermo, Italy

<sup>b</sup>Dipartimento dell' Energia, Ingegneria, dell'Informazione e Modelli Matematici - Università di Palermo, Viale delle Scienze Ed. 6, 90128 Palermo, Italy)  
[alessandro.tamburini@unipa.it](mailto:alessandro.tamburini@unipa.it)

Solid-liquid mixing within tanks agitated by stirrers can be easily encountered in many industrial processes. It is common to find an industrial tank operating at an impeller speed  $N$  lower than the minimum agitation speed for the suspension of solid particles: under such conditions the distribution of solid-particles is very far from being homogeneous and very significant concentration gradients exist. The present work evaluates the capability of a Computational Fluid Dynamics (CFD) model to reliably predict the particle distribution throughout the tank under either partial or complete suspension conditions. A flat bottomed baffled tank stirred by a Rushton turbine was investigated. Both transient and steady state RANS simulations of the stirred tank were performed with the commercial code CFX4.4. The Eulerian-Eulerian Multi Fluid Model along with the  $k-\epsilon$  turbulence model was adopted. Either the Sliding Grid or the Multiple Reference Frame technique was employed to simulate the impeller to baffle relative rotation. Inter-phase momentum exchange terms were approximated only by the inter-phase drag forces. Literature experimental data were used for the model validation. Results show that the model along with the Sliding Grid technique can reliably predict the experimental particle distribution at all investigated impeller speeds. Radial gradients of solids concentration, usually neglected in the literature, were found to be significant in the presence of unsuspended solid particles (partial suspension conditions).

### 1. Introduction

Industrial tanks devoted to the mixing of solid particles into liquids are often operated at an impeller speed  $N$  lower than the minimum one allowing the suspension of particles ( $N_{js}$ ). Most solid-liquid mixing operations require the knowledge of  $N_{js}$  and/or of the amount of solids suspended at different agitation speeds below  $N_{js}$  (i.e the suspension curve). In many cases it is also required that information is gained on the quality of the solids distribution within the tank, since the particle distribution may largely affect the process performance. In such cases, a reliable prediction of the solids distribution is of crucial importance for an accurate design and testing of the pertaining solid-liquid stirred systems (Tamburini et al., 2009a). Also, the knowledge of local particle concentration fields is essential to allow a sound understanding of the mechanisms of solids suspension and dispersion occurring inside these systems (Tamburini et al., 2013). Surprisingly, it is not easy to find such data in the literature for partial suspension conditions, notwithstanding the interest expressed so far at the industrial level for this particular regime.

Experimental data on particle distribution into a liquid within a stirred tank are usually presented in the form of axial and radial profiles of solids concentration. In the literature it is easy to find similar local data, especially when the solids concentration is measured by intrusive techniques making use of a probe. Sometimes local information is assumed to be valid for the entire radial direction (Barresi and Baldi, 1987; Shamlou and Koutsakos, 1989; Micheletti et al., 2003) or even for the whole horizontal plane (e.g. this is

the case of measurements taken by the light attenuation technique, Magelli et al., 1990). This is justified by assuming that either the radial gradients of solid concentration or both radial and azimuthal gradients are negligible. The distribution of solid particles in a stirred vessel is a quite complex function of the velocity field, turbulence characteristics and liquid-particle interactions. Thus, the soundness of the former approximation depends on several factors, such as geometrical configuration (Micale et al., 1999) and suspension properties: for example (i) radial impellers provide larger concentration gradients than axial impellers and (ii) the higher the particle size and concentration, the higher the concentration gradients (Barresi and Baldi, 1987).

The present work is devoted to the investigation via CFD of the particle distribution in a dense suspension ranging from partial to complete suspension conditions. In particular, the CFD model by Tamburini et al. (2011a) is the only one purposely developed to deal with partial suspension conditions. It has been fully validated in previous works and found to reliably predict integral data in the form of (i) suspension curves (Tamburini et al., 2011a), (ii)  $N_{js}$  (Tamburini et al., 2012a) and (iii) impeller speed for sufficient suspension conditions (Tamburini et al., 2012b). Such essential data concerning the particle suspension phenomenon, however, do not provide any information on local details since they are intrinsically lumped. Investigation of particle distribution completes the description of the solid-liquid suspension by adding a further level of detailed information throughout the whole vessel volume. Here, the model by Tamburini et al. (2011a) is further tested in order to evaluate its capability to deal with local particle concentration distribution under incomplete suspension conditions. Notably, to the authors' knowledge, no literature work has addressed this specific topic so far: all the CFD models proposed in the literature are generally validated against experimental axial profiles of solids concentration collected at  $N$  equal or higher than  $N_{js}$ .

## 2. Systems under investigation

The experimental data to be simulated derive from the literature (Micheletti et al., 2003). Only some details are reported in the following, full details can be found in the pertinent paper. The experimental system simulated consisted of a cylindrical flat bottomed baffled tank with vessel diameter  $T=0.29$  m and total liquid height  $H=T$ . A standard six-bladed Rushton turbine with  $D=T/3$  was used and set at a distance from the vessel bottom equal to  $T/3$ . Deionised water ( $\rho_\alpha = 1000$  kg/m<sup>3</sup>) and mono-dispersed glass particles ( $d_p = 600-710$   $\mu\text{m}$ ;  $\rho_\beta = 2470$  kg/m<sup>3</sup>) were employed. Solid loading was equal to 9.2%  $V_{\text{solid}}/V_{\text{total}}$  ( $r_\beta^{\text{av}}$ ). Maximum physically allowed packing value of the particle bed was estimated to be 60%  $V_{\text{solid}}/V_{\text{bed}}$  ( $r_\beta^{\text{packed}}$ ).

## 3. Modelling and numerical details

Only a short description of the adopted CFD model will be given in the following; further details can be found in Tamburini et al. (2011a). All CFD simulations were carried out by using the commercial code *CFX4.4* (Ansys®). The Eulerian-Eulerian Multi Fluid Model was adopted to simulate the two-phases which are treated as two interpenetrating continua. The relevant continuity and momentum balance equations are reported below.

$$\rho_i \frac{\partial}{\partial t}(r_i) + \rho_i \vec{\nabla} \cdot (r_i \vec{U}_i) = 0 \quad (1)$$

$$\frac{\partial}{\partial t}(r_i \rho_i \vec{U}_i) + \vec{\nabla} \cdot \left\{ r_i \left[ \rho_i \vec{U}_i \otimes \vec{U}_i - (\mu_i + \mu_i) \left( \vec{\nabla} \vec{U}_i + (\vec{\nabla} \vec{U}_i)^T \right) \right] \right\} = r_i (\rho_i \vec{g} - \vec{\nabla} P) + \vec{F}_{i,j} \quad (2)$$

where  $r$  is volumetric fraction,  $\rho$  the density and  $U$  the mean velocity,  $i$  indicates the liquid or solid phase,  $g$  the gravity acceleration,  $\mu$  the viscosity,  $P$  the pressure (the solid and the liquid phases share the same pressure field) and  $F$  is the inter-phase drag force (clearly  $F_{i,j} = -F_{j,i}$ ). All other inter-phase forces were neglected as suggested by the literature for density ratio between the two phases higher than 2. No turbulence was assumed in the solid phase: this choice ("*asymmetric turbulence modelling*") was found suitable to model dense solid-liquid suspensions in stirred tanks under partial-to-complete suspension regimes (Tamburini et al., 2011a,b; Tamburini et al., 2012a,b): in particular, the Asymmetric  $k-\epsilon$  turbulence model (Tamburini et al., 2011a) was employed here. A molecular viscosity equal to the liquid one was chosen for the solid phase as suggested by the literature (Tamburini et al., 2011a,b).

A standard formulation was adopted for the drag force:

$$\vec{F}_{\alpha\beta} = \left[ \frac{3}{4} \frac{C_D}{d_p} r_\beta \rho_\alpha |\vec{U}_\beta - \vec{U}_\alpha| \right] (\vec{U}_\beta - \vec{U}_\alpha) \quad (3)$$

where,  $C_D$  is drag coefficient. Particle drag coefficient  $C_D$  was considered variable in each cell in relation to the slip velocity between phases in accordance with Clift et al. correlation (1978). Free-stream turbulence influence upon drag coefficient was accounted for by employing the correlation by Brucato et al. (1998). The Excess Solid Volume Fraction Correction (ESVC) algorithm (Tamburini et al., 2009b) was adopted to avoid that  $r_\beta^{\text{packed}}$  could be largely exceeded during the simulations.

As far as the treatment of the impeller-baffle relative rotation is concerned, both the steady state Multiple Reference Frame (MRF) and the time dependent Sliding Grid (SG) algorithm (more accurate but much more computationally demanding) were adopted in the present work.

In MRF simulations typically 12000 SIMPLEC iterations were found to be sufficient to allow variable residuals to settle to very low values for all the cases investigated. As far as the SG simulations are concerned, 100 full revolutions were considered sufficient to reach steady state conditions in all cases, coherently with what is reported by the literature for similar systems (Tamburini et al., 2009a and 2011a). The number of SIMPLEC iterations per time step was set to 30 to allow residuals to settle before moving to the next time step.

The SIMPLEC algorithm was adopted to couple pressure and velocity. Central differences were employed for all diffusive terms. The hybrid-upwind discretization scheme was employed for the convective terms. In accordance with the system's axial symmetry, only one half of the tank was included in the computational domain and two periodic boundaries were imposed along the azimuthal direction. The structured grid chosen for the discretization of this half-tank encompasses 74592 cells distributed as  $72 \times 37 \times 28$  along the axial, radial and azimuthal direction respectively. Some simulations were carried out also by employing a 8 times finer grid: quite identical results ( $r_\beta$  axial profiles) were obtained by employing the two grids.

## 4. Results and discussion

### 4.1 Impeller modelling technique

Figure 1 reports the comparison between the experimental local profiles of  $r_\beta$  measured by Micheletti et al. (2003) and the corresponding CFD predictions provided by the Tamburini et al. model (2011a). Notably, these CFD simulations represent the first attempt in the literature to predict the solid distribution in a stirred tank under partial suspension conditions.

At 400 RPM (i.e. an  $N \ll N_{js}$ ), the model along with the SG algorithm manages to predict with high accuracy the experimental profile: only slight differences among CFD results and experiments are observable. The presence of particles near the vessel bottom with a volumetric fraction corresponding to the maximum allowed one (i.e.  $r_\beta^{\text{packed}} = 0.6$ ) is very well predicted by CFD simulations thus confirming the effectiveness of the ESVC algorithm. Actually, the CFD simulation for the 400rpm cases slightly underestimates the particle concentration in the upper region of the vessel ( $Z \geq 0.4$ ) with respect to the experimental data. The steady state simulation performed via the MRF approach for the same test case provides results very similar to the SG ones, especially over the impeller plane, conversely, some differences can be observed just over the vessel bottom (i.e.  $Z/H < 0.1$ ). At 500 RPM the SG-model follows well the experimental data especially in the lower part of the vessel. Only at the top of the vessel, the experimental solids concentration is underestimated by the model. Also MRF results follow the shape of the experimental profile, but exhibit a discrepancy from experimental data larger than the SG results. As concerns the unsuspended particle distribution throughout the whole tank, clearly the amount of sediment is reduced as  $N$  increases from 400rpm to 500rpm. At 600 RPM the SG-model predictions show an underestimation of experimental data below the impeller plane. As far as the upper part of the vessel is concerned only slight differences between experimental and computational data are observable. Again, a non negligible difference between the SG and the MRF profiles can be observed especially above the impeller plane: even in this case, the results relevant to the SG technique are in a better agreement with the experimental data. At 700 RPM a good agreement between the experimental profile and the SG-model predictions is observable above the impeller plane: only the experimental point at the highest elevation is not well predicted by the CFD simulation. Below the impeller plane, the figure shows an underestimation of experimental data whose amplitude appears to be lower than in the 600 RPM case. The MRF model results exhibit a larger underestimation of the experimental data below the impeller plane and a wrong shape of the concentration profile above it. The  $N_{js}$  calculated by Micheletti et al. (2003) by means of

Zwietering's correlation was found to be 988 RPM so that all the experimental profiles discussed so far are relevant to partial suspension conditions. On the other hand, the impeller speed of 1100 RPM is higher than  $N_{js}$  but lower than the speed necessary for the achievement of homogeneous suspension conditions: in other words, the case of 1100 RPM is representative of the commonly investigated regime of complete suspension. A very good agreement between the SG-model prediction and the experimental profile is observable at this  $N$ . Notably, the under-predictions formerly seen below the impeller plane for the 600 RPM and 700 RPM cases completely disappear at 1100 RPM. Only the experimental point corresponding to the impeller plane height is slightly under-predicted. The MRF-model predictions are very similar to the SG-model ones, even if larger discrepancies (both below and above the impeller plane) can be observed. Tamburini et al. (2011a) found that very similar results are provided by SG and MRF in terms of mass fraction of solids resting on the bottom. Conversely differences in the local axial  $r_\beta$  profile were found at all speeds in the present work, as shown in Figure 1. Summarizing, it can be stated that for the case of partial suspension conditions, integral data can be predicted with very similar accuracy by SG and MRF simulations, while local information is better predicted by employing the SG approach. This is not surprising, since the CFD prediction of local data concerning solid concentration values at different vessel heights allegedly requires a more accurate calculation. As a matter of fact, in accordance with the relevant literature (Panneerselvam et al., 2008), a transient CFD simulation approach based on the fully predictive SG algorithm accounts for the temporal variations in the mixing tank thus providing better predictions of the liquid flow field and solid suspension than the MRF steady state framework.

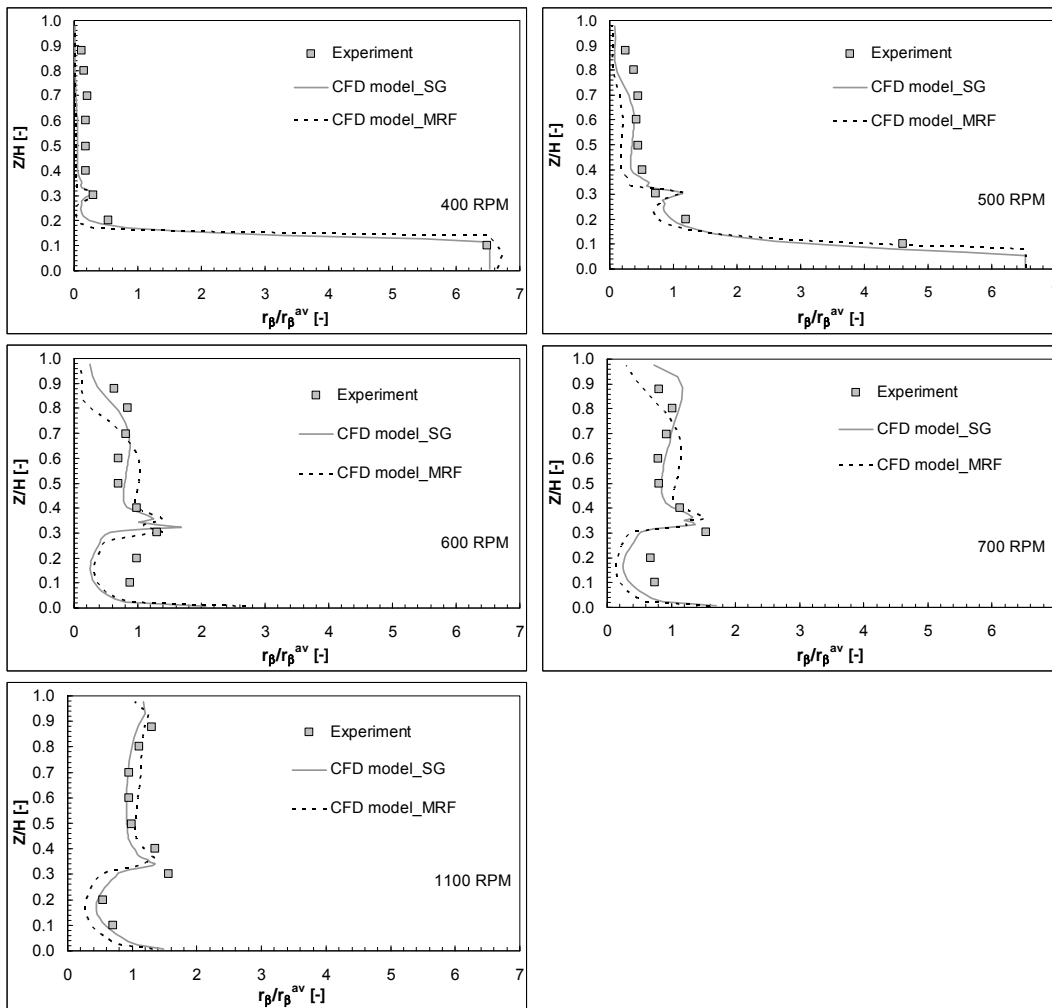


Figure 1: SG/MRF simulations versus experimental (Micheletti et al., 2003) local (midway between subsequent baffles and at a radial position  $R = 0.35T$ ) axial profiles of normalized  $r_\beta$  at some different impeller speeds ( $N_{js} = 988$  RPM).

#### 4.2 Radial profiles of particle concentration

All the axial profiles presented so far refer to a specific radial and azimuthal location: in the literature it is easy to find similar local data, especially when the solids concentration is measured by intrusive techniques making use of a probe. Such local axial data are often extended to the total radial direction. In order to qualitatively evaluate the reliability of this approximation, in Figure 2 the local axial profiles already shown in Figure 1 are compared with corresponding radially averaged profiles.

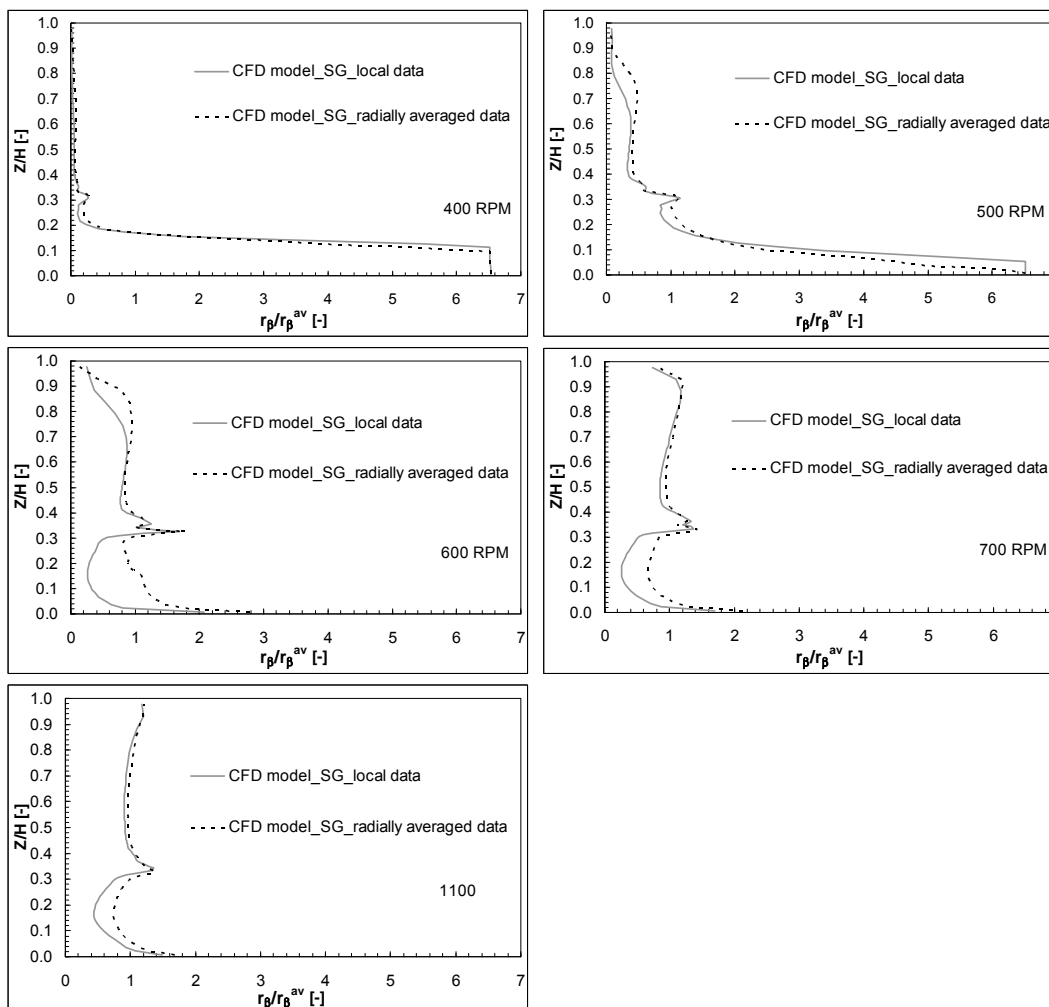


Figure 2: Comparison between local and radially averaged SG axial profiles of  $r_\beta$  (midway between subsequent baffles and at  $R = 0.35T$ ) at some different impeller speeds.

At 400 RPM the tank is practically divided in two parts separated by an almost flat interface: the upper part is full of liquid only, the lower one is characterized by the presence of still solids exhibiting a  $r_\beta = r_\beta^{\text{packed}}$ . In these conditions, radial gradients may be important only in the proximity of the interface between these two zones, while they can be reasonably neglected in the rest of the tank. At 500 RPM, three different zones separated by two widespread interfaces can be recognized (not shown here): the sediment zone, the suspension zone and the almost-clear liquid layer zone. As concerns the sediment-suspension interface, at this higher agitation speed the sediment is profiled by the liquid flow and exhibits a more complex shape. This three-dimensional shape of the sediment-suspension interface makes the assumption of negligible radial and azimuthal  $r_\beta$  gradients less reliable. The local and the radially averaged profiles mainly differ in the proximities of the two widespread interfaces (sediment-suspension and suspension-almost clear liquid layer). At larger impeller speeds (i.e. 600 RPM and 700 RPM, lower than  $N_{js}$ ), the difference between the local and the radially averaged profiles decreases as  $N$  increases both in the upper and in the lower part of the vessel. As regards the upper part, a negligible difference between

the two profiles can be seen when many particles reach the vessel top (i.e. at 700 RPM) causing the liquid layer to be completely replaced by the suspension and the suspension-liquid layer interface to disappear. A similar reduction of the difference between the two profiles with  $N$  can be seen below the impeller plane since the presence of the sediment leads to a strong concentration gradient along the radial direction in both cases. At impeller speeds higher than  $N_{js}$  (i.e. 1100 RPM) all particles are suspended and no fillet is present thus resulting in very similar profiles with slight differences located only in the lower part of the tank.

## 5. Conclusions

Reynolds Average Navier Stokes (RANS) simulations of dense solid-liquid suspensions within a flat bottomed vessel stirred by a standard Rushton turbine were performed with a finite volume code by adopting the fully predictive Eulerian-Eulerian Multi Fluid Model in conjunction with the  $k-\varepsilon$  turbulence model for the continuous (liquid) phase. The specific modelling and numerical details employed were those adopted in Tamburini et al. (2011a) to predict global quantities linked to the particle suspension phenomenon. Here, this model was further tested in order to evaluate its capability of predicting also the three-dimensional particle distribution phenomenon. Both the time-dependent Sliding Grid (SG) method and the steady state Multiple Reference Frame (MRF) technique were used.

Results showed that experimental local axial profiles of solid concentrations (a typical information characterizing the particles distribution) at different impeller speeds ranging from partial to complete suspension conditions can be predicted with a high accuracy. In particular the transient SG simulation results were found to better predict the experimental data than the steady state MRF simulations.

Although the radial profiles of solid concentrations are often neglected in the literature, the present results showed that this approximation is unjustified in some cases and/or in some zones of the tank, especially under partial suspension conditions in which unsuspended particles are present on the vessel bottom.

## References

- Barresi A., Baldi G., 1987, Solid dispersion in an agitated vessel, *Chem. Eng. Sci.*, 42, 2949-2956.
- Brucato, A., Grisafi, F., Montante, G., 1998, Particle drag coefficients in turbulent fluids, *Chem. Eng. Sci.*, 53, 3295-3314.
- Magelli F., Fajner D., Nocentini M., Pasquali G., 1990, Solid distribution in vessels stirred with multiple impellers. *Chem. Eng. Sci.*, 45, 615-625.
- Micale G., Brucato A., Grisafi F., Ciofalo M., 1999, Prediction of flow fields in a dual-impeller stirred vessel, *AIChE Journal*, 45, 445-464.
- Micheletti M., Nikiforaki L., Lee K.C., Yianneskis M., 2003, Particle concentration and mixing characteristics of moderate-to-dense solid-liquid suspensions, *Ind. Eng. Chem. Res.*, 42, 6236-6249.
- Panneerselvam R., Savithri S., Surender G.D., 2008, CFD modeling of gas-liquid-solid mechanically agitated contactor, *Chemical Engineering Research Design*, 86, 1331-1344.
- Shamlou P. A., Koutsakos E., 1989, Solids suspension and distribution in liquids under turbulent agitation, *Chemical Engineering Science*, 44, 529 – 542.
- Tamburini, A., Gentile, L., Cipollina, A., Micale, G., Brucato, A., 2009a. Experimental investigation of dilute solid-liquid suspension in an unbaffled stirred vessels by a novel pulsed laser based image analysis technique, *Chemical Engineering Transactions*, 17, 531-536.
- Tamburini A., Cipollina A., Micale G., Ciofalo M., Brucato A., 2009b, Dense solid-liquid off-bottom suspension dynamics: simulation and experiment, *Chem. Eng. Res. Des.*, 87, 587-597.
- Tamburini A., Cipollina A., Micale G., Brucato A., Ciofalo, M., 2011a, CFD simulations of dense solid-liquid suspensions in baffled stirred tanks: predictions of suspension curves, *Chem. Eng. J.*, 178, 324-341.
- Tamburini A., Cipollina A., Micale G., 2011b, CFD simulation of solid liquid suspensions in baffled stirred vessels below complete suspension speed, *Chemical Engineering Transactions*, 24, 1435-1440.
- Tamburini A., Brucato A., Cipollina A., Micale G., Ciofalo M., 2012a, CFD predictions of sufficient suspension conditions in solid-liquid agitated tanks, *Int. J. Nonlinear Sci. Num. Sim.*, 13, 427-443.
- Tamburini, A. Cipollina A., Micale G., Brucato A., Ciofalo M., 2012b. CFD simulations of dense solid-liquid suspensions in baffled stirred tanks: prediction of the minimum impeller speed for complete suspension. *Chem. Eng. J.*, 193-194, 234-255.
- Tamburini A., Cipollina A., Micale G., Brucato A., 2013, Particle distribution in dilute solid liquid unbaffled tanks via a novel laser sheet and image analysis based technique, *Chem. Eng. Sci.*, 87, 341-358.